

# Time-of-Flight Tip-Clearance Measurements

H.S. Dhadwal  
Integrated Fiber Optic Systems, Inc., Stony Brook, New York

A.P. Kurkov and D.C. Janetzke  
Glenn Research Center, Cleveland, Ohio

## The NASA STI Program Office . . . in Profile

Since its founding, NASA has been dedicated to the advancement of aeronautics and space science. The NASA Scientific and Technical Information (STI) Program Office plays a key part in helping NASA maintain this important role.

The NASA STI Program Office is operated by Langley Research Center, the Lead Center for NASA's scientific and technical information. The NASA STI Program Office provides access to the NASA STI Database, the largest collection of aeronautical and space science STI in the world. The Program Office is also NASA's institutional mechanism for disseminating the results of its research and development activities. These results are published by NASA in the NASA STI Report Series, which includes the following report types:

- **TECHNICAL PUBLICATION.** Reports of completed research or a major significant phase of research that present the results of NASA programs and include extensive data or theoretical analysis. Includes compilations of significant scientific and technical data and information deemed to be of continuing reference value. NASA's counterpart of peer-reviewed formal professional papers but has less stringent limitations on manuscript length and extent of graphic presentations.
- **TECHNICAL MEMORANDUM.** Scientific and technical findings that are preliminary or of specialized interest, e.g., quick release reports, working papers, and bibliographies that contain minimal annotation. Does not contain extensive analysis.
- **CONTRACTOR REPORT.** Scientific and technical findings by NASA-sponsored contractors and grantees.

- **CONFERENCE PUBLICATION.** Collected papers from scientific and technical conferences, symposia, seminars, or other meetings sponsored or cosponsored by NASA.
- **SPECIAL PUBLICATION.** Scientific, technical, or historical information from NASA programs, projects, and missions, often concerned with subjects having substantial public interest.
- **TECHNICAL TRANSLATION.** English-language translations of foreign scientific and technical material pertinent to NASA's mission.

Specialized services that complement the STI Program Office's diverse offerings include creating custom thesauri, building customized data bases, organizing and publishing research results . . . even providing videos.

For more information about the NASA STI Program Office, see the following:

- Access the NASA STI Program Home Page at **<http://www.sti.nasa.gov>**
- E-mail your question via the Internet to **[help@sti.nasa.gov](mailto:help@sti.nasa.gov)**
- Fax your question to the NASA Access Help Desk at (301) 621-0134
- Telephone the NASA Access Help Desk at (301) 621-0390
- Write to:  
NASA Access Help Desk  
NASA Center for Aerospace Information  
7121 Standard Drive  
Hanover, MD 21076



# Time-of-Flight Tip-Clearance Measurements

H.S. Dhadwal

Integrated Fiber Optic Systems, Inc., Stony Brook, New York

A.P. Kurkov and D.C. Janetzke

Glenn Research Center, Cleveland, Ohio

Prepared for the  
35th Joint Propulsion Conference and Exhibit  
sponsored by the AIAA, ASME, SAE, and ASEE  
Los Angeles, California, June 20-24, 1999

National Aeronautics and  
Space Administration

Glenn Research Center

Available from

NASA Center for Aerospace Information  
7121 Standard Drive  
Hanover, MD 21076  
Price Code: A03

National Technical Information Service  
5285 Port Royal Road  
Springfield, VA 22100  
Price Code: A03

# TIME-OF-FLIGHT TIP-CLEARANCE MEASUREMENTS

H.S. Dhadwal  
Integrated Fiber Optic Systems, Inc.  
Stony Brook, New York

A.P. Kurkov and D.C. Janetzke  
National Aeronautics and Space Administration  
Glenn Research Center  
Cleveland, Ohio

## Abstract

In this paper a time-of-flight probe system incorporating the two integrated fiber optic probes which are tilted equally relative to the probe holder centerline, is applied for the first time to measure the tip clearance of an advanced fan prototype. Tip clearance is largely independent of the signal amplitude and it relies on timing measurement. This work exposes optical effects associated with the fan blade stagger angle that were absent during the original spin-rig experiment on the zero stagger rotor. Individual blade tip clearances were measured with accuracy of  $\pm 0.127$ -mm ( $\pm 0.005$ -in). Probe features are discussed and improvements to the design are suggested.

## Introduction

In an earlier paper Dhadwal and Kurkov<sup>1</sup> described the dual-beam time-of-flight tip-clearance probe and applied it to measure controlled spacing between the probe face and a specially designed non-deflecting rotor, Fig. 1. The spacing measurement was performed in a direction perpendicular to the plane of rotation near the outer diameter of the rotor in a vacuum spin rig. As depicted in Fig. 1, the plane of the rotation was horizontal, and probe was mounted on a vertical traversing stage so that the clearance between the tip of the probe and the rotor could be varied at will. This spacing measurement simulates the tip clearance measurement and it relies on the timing of the interval that it takes a rotor tooth (at the tip of its radius) to cross the space between the two beams generated by the two independent integrated fiber-optic probes. The two probes were tilted relative to each other in the plane perpendicular to the centerline radius of the rotor tooth.

In this paper a symmetric dual-probe arrangement, in which the two integrated fiber optic probes are tilted equally relative to the probe holder centerline, is

applied to measure the tip clearance of an advanced fan prototype. Figure 2 is a photograph of the probe holder. The design of a 3.175 mm (0.125 in) integrated fiber optic probe was reported in previous papers (Dhadwal and Kurkov<sup>1</sup>, and Dhadwal et.al.<sup>2</sup>)

## Tip Clearance Measurement

Figure 3 presents a sketch of a symmetric tip-clearance probe that defines all the pertinent geometrical parameters. The two legs of the symmetric probe assembly are actually separate integrated fiber-optic probes designated as P7 and P1. Because the face of the probe assembly was slightly recessed below the rub strip, its precise location relative to the rub strip diameter was difficult to determine. Therefore, in addition to determining clearances relative to the face of the probe they were also evaluated relative to a reference speed of 1000 rpm. The change in the tip clearance in the Z direction when speed is increased corresponds to a shift in the blade tip trajectory from  $\overline{DE}$  to  $\overline{FG}$ . Blade radii R's are used to approximate  $\overline{DE}$  and  $\overline{FG}$  with arcs as shown in the sketch, where  $\alpha$ 's are in radians. When  $\alpha$ 's are converted into degrees, the shift in the Z direction can be expressed as

$$\Delta Z = -\frac{\pi}{360 \tan \phi} (R_2 \alpha_2 - R_1 \alpha_1) \quad (1)$$

where subscript 1 corresponds to 1000 rpm, subscript 2 to either 4460 or 7950 rpm, and the half included angle  $\phi$  is 20 degrees. The clearance gap evaluated in the negative Z direction relative to the face of the probe is given by

$$Z_g = -Z = \frac{\overline{BC} - \overline{DE}}{2 \tan \phi}$$

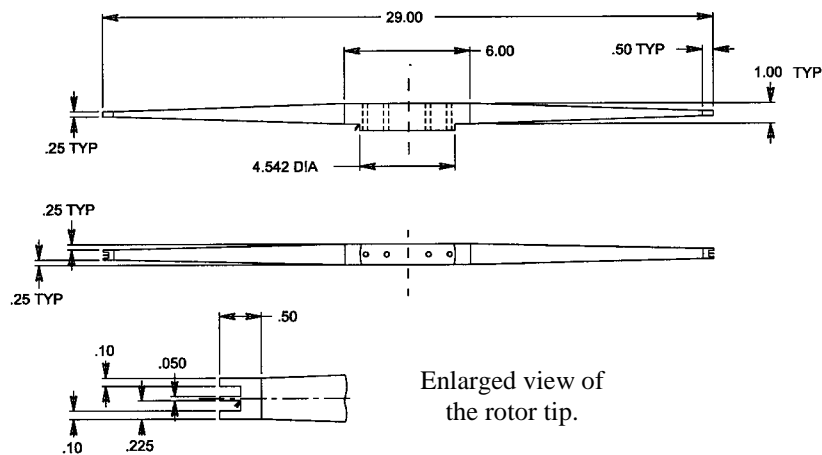


Figure 1.—Non-deflecting titanium rotor for optical probe calibrations.

where the beam separation distance at the face of the probe,  $\overline{BC}$ , is evaluated from probe calibration, and the distance  $\overline{DE}$  corresponds to any speed and is approximated as an arc, as in the previous equation.

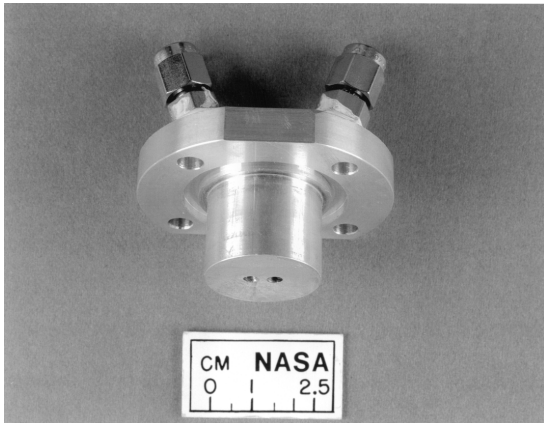


Figure 2.—Probe holder.

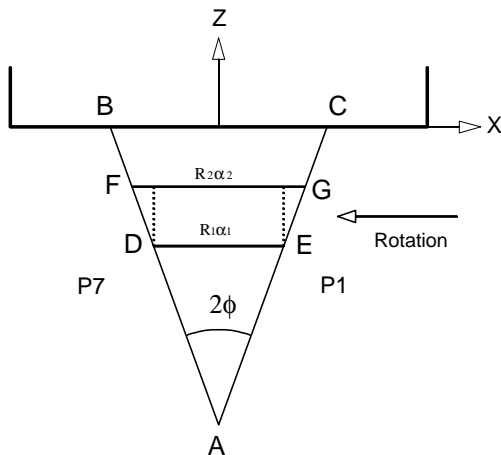


Figure 3.—Probe P7 and P1 beam geometry.

The digitized traces for a particular blade (number 6) are illustrated in Figs. 4 and 5. Note that the probe P1 has a lower noise floor than the probe P7. This occurs, probably, because the probe P7 is swept in such a way that it faces an approaching blade, Fig. 3, and consequently, it picks-up some of the reflected light from a blade prior to its encounter with the beam. The probe P1, on the other hand, is swept in such a way that it minimizes light pickup from an approaching blade. The logical choice for a trigger point for the probe P1 is the start of the rise of signal amplitude (i.e., the leading corner of the trace). Because of the relatively low noise and a fairly sharp rise in amplitude this is also a reasonable choice for probe P7 as well; however, one must ensure that the trigger point is above the expected noise level. In this way, the dependence of the trigger point on the signal amplitude is minimized.

Comparison of the leading and trailing slopes expressed in terms of spatial coordinates at low and high speeds in Figs. 4 and 5, shows that they are invariant with speed, indicating that the signal response time was sufficiently high to factor out possible speed dependence of the signals when they are viewed in spatial coordinates. The digitizing rate for 7950 rpm traces was 50MHz; for 1000 rpm, 5MHz; and for the 4460 rpm it was 25MHz. The resolution was 12 bits for all speeds.

A reference once-per-revolution signal was generated by reflecting a He-Ne laser beam from the mirror mounted on the shaft. The central rays from the reflected beam passed through a small aperture to narrow the beam which then impinged on an avalanche photodiode. This signal was used to sort the continuous stream of data into single revolution segments, enabling conversion of the time coordinate into a spatial coordinate—such as the angle associated with circumferential blade-tip orbit. Specifically, since the

P1 and P7 signals were digitized simultaneously, angle  $\alpha$  (Fig. 3) can be determined at a given speed by subtracting P7 from P1 point counts\* (relative to the once-per-revolution signal), dividing the difference by the revolution count associated with the particular trace, and multiplying the result by 360.

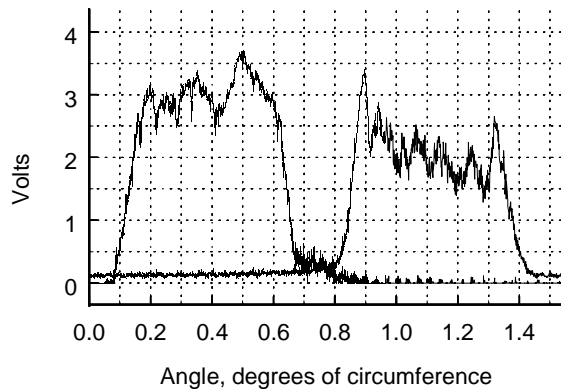


Figure 4.—Probe P7 and P1 traces at 1006.7 1.

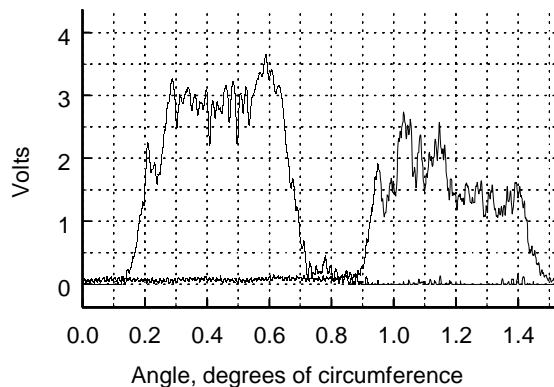


Figure 5.—Probe P7 and P1 traces at 7952.2 rpm.

In order to evaluate this system in a controlled environment, a test was performed in the NASA's spin-rig facility using a specially designed non-deflecting rotor, Fig. 1. It consisted of a tapered titanium bar, 73.66-cm (29-in) in diameter with three teeth on each end. The middle tooth measuring 1.295-mm (0.051-in) in width simulated a blade tip. The bar and measuring teeth were in a horizontal plane in the spin rig and the axis of rotation was vertical. The probe was mounted on an optical stage so that the rotor tooth trajectory traverses P1-P7 plane and is perpendicular to the radius extending through the centerline of the middle tooth. The clearances were set dynamically with accuracy of better than 0.025 mm (0.001 in).

\* We have retained digitized point counts as units for the independent variable, rather than converting these units into time units.

To calibrate the tip clearance probe, relative to the values computed from Eq.2, the clearance gap was varied remotely while speed was kept constant. The results are illustrated in Fig. 6. They are consistent up to 2000 rpm. Because the comparison of the signals at low and high speeds revealed no degradation with speed, as shown in Figs. 4 and 5 for the wind tunnel data, the inconsistencies at 4000 and 8000 rpm, apparently, result from an axial motion of the rotor. In Fig. 7, 500 rpm data were used to obtain the least square linear fit to the measured points. (Any other low-speed set of data at or below 2000 rpm could have been used as well). The tip clearance relative to the face of the probe can be expressed as

$$Z_g = (0.235911 - 0.251641 * \alpha) / (1 - 0.022752 \alpha) \quad (3)$$

where the appropriate rotor radius was used and angle  $\alpha$  was expressed in degrees. The non-linear term in the denominator arises because of the slight dependence of  $R_2$  on  $\Delta Z$  and, therefore, on  $\alpha$ . This relationship was used to obtain clearances for the fan rotor tested in the wind tunnel.

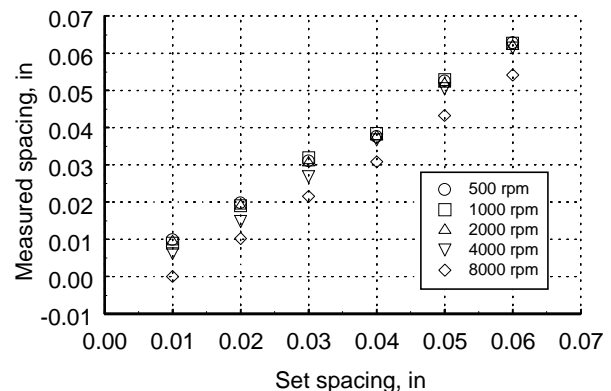


Figure 6.—Probe calibration, full speed range.

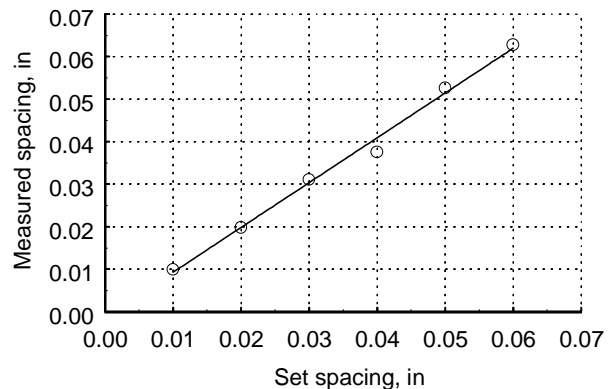


Figure 7.—Linear least square fit, 500 rpm.

The tip clearance relative to the face of the probe,  $Z_g$ , for 1000, 4460, and 7950 rpm is plotted in Fig. 8. Only half of the rotor blades (3 to 11) are included in the figure, because of the on-board memory limitation of the A/D board. For the two higher speeds, clearances relative to 1000 rpm are presented in Figs. 9 and 10.

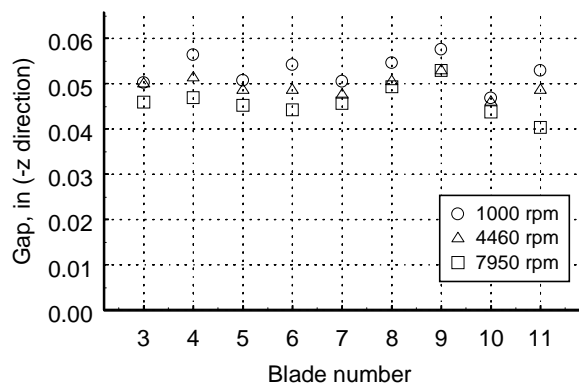


Figure 8.—Clearance gap relative to the probe face.

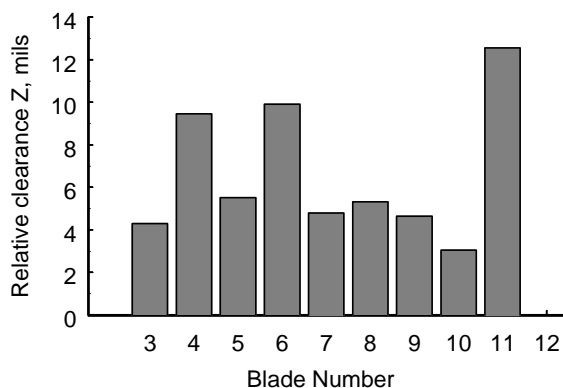


Figure 9.—Clearance at 7952.2 rpm relative to 1006.7.

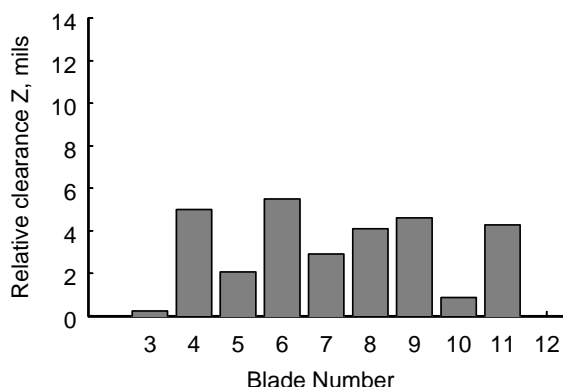


Figure 10.—Clearance at 4464 rpm relative to 1006.7.

Currently, the accuracy of measurements is about  $\pm 0.127$  mm ( $\pm 0.005$  in) and is essentially limited by the signal to noise ratio of the probe (P7) that faces the approaching blade (Fig. 3). To improve the signal-to-noise ratio and therefore enhance the consistency of the trigger point, Dhadwal and Kurkov<sup>1</sup> tested an asymmetric configuration of the tip clearance probe that replaces the P7 (Fig. 3) leg of the current probe with a probe that is lined-up with the Z axis. The results of the tests in the vacuum spin rig indicate a noticeable improvement in the quality of the signal for this probe. Further improvement of the signals can be achieved by increasing the laser power and then operating in the non-linear range of the receiver module (Dhadwal and Kurkov<sup>1</sup>).

To achieve the optimum calibration for the symmetric probe in the spin rig, the negative (or falling) slope of the P7 signal, rather than positive (as for P1 signal) was chosen. To account for this fact, the results were subsequently compensated by subtracting the number of counts corresponding to the known thickness of the middle tooth of the rotor. Note that this procedure cannot be applied to the fan rotor test because there the blade thickness cannot be assumed to be constant. However, the background level of optical noise is somewhat alleviated there by the blade stagger. In the future, it is also expected that the nonsymmetrical probe design will additionally improve quality of the positive slope of the P7-leg signal.

Although the described method of measurements is reasonably independent of the pulse amplitude, the timing measurements are still subject to errors caused by possible surface irregularities (such as nicks) at the blade pressure- and suction-surface corners in the beam-plane cross-section. A change in timing measurement from these imperfections is indistinguishable from that caused by actual change in the tip clearance. In order to minimize the impact of the surface irregularities, one could perform a series of measurements over a small range of rotational speeds bracketing the desired speed. Because the sensor is stationary and the blade tip deforms slightly in response to the change in operating conditions associated with the slight change in speed, different points on blade edges will be intercepting the beams. By averaging the timing measurements over this speed range, the impact of surface imperfections should be significantly reduced.

This problem can also be resolved in another way, by incorporating probe actuation in the radial direction as discussed in the following section.

### The Scanning Probe

Figure 11 illustrates the measurement principle. The new probe head integrates the two fiber-optic probes into one compact unit. The beam separation and the standoff distance between the base of the probe and the beam intersection are much smaller than in the time-of-flight probe, and the probe can be traversed in the radial direction with a remote-controlled actuator. The object is to position the intersection of two beams onto a passing blade tip, by establishing confluence of the two pulses associated with each beam of light, as illustrated in the lower part of Fig. 11. In regions I and II, there are two closely spaced pulses each associated with a separate beam. As the probe is advanced in the positive  $X$  direction, the separation between the two pulses decreases when a blade tip is in region II, whereas it increases it is in region I. The two pulses merge in the focal region. The goal is to attain the minimum width of the merged pulse signature on the oscilloscope by manipulating the probe actuator. The tip clearance at a given operating condition can be simply deduced from the amount of probe travel from the established position of the probe face relative to the inner edge of the rub strip, and the statically calibrated focal length  $X_f$ . The pulse coincidence can be established by displaying the two probe signals on a deep-memory, high frequency, digital oscilloscope. The probe actuation control can be performed either manually via a remote controller with a graphical user interface, or automatically, by programming a microcomputer and accomplishing pulse coincidence detection through a suitable algorithm. The oscilloscope should be triggered with a once-per-revolution pulse generated by an optical probe.

As an alternative to capturing pulse coincidence for each blade in turn, one could first obtain the maximum tip clearance, which occurs for a blade that requires the actuator to be in the extreme right position in Fig. 11. Once it is found, a controlled radial sweep moving the actuator away from the blades would suffice to catch the clearance of all blades. The sorting of blades into separate revolutions and searching for pulse coincidences would be performed in software on a microcomputer. The clearance would fall out from correlating the position of the actuator to the specific pulse coincidences.

Because the width of the focal region is much smaller than the blade width, as the beam coincidence is approached, the receiving fibers from one probe will receive some light transmitted by the other probe, in addition to the light transmitted by the particular's probe single-mode fiber. Thus, the source of the displayed signals will be somewhat uncertain; however,

it follows from Fig. 11 that in region I, the upper (or the pressure) surface of the blade will be the one that generates the rising slope of the signal from the light emanating strictly from probe P2. Similarly, the falling slope of the signal in region I is strictly generated from the light passed by probe P1, as the lower (or the suction) surface of the blade leaves this region. Thus, the pulse edges are well defined, all the way to the minimum pulse width. Because the cross section of the blade tip as traced by a stationary beam changes as the blade deforms, the minimum pulse width will change with operating conditions; however, the minimum pulse width will always be associated with the focal plane. The design of the probe actuation mechanism should be integrated with probe seal design, which will dictate the required force to be generated by a servomotor. The employment of a servomotor guarantees the precise knowledge of the radial position of the probe. Kurkov and Dhadwal<sup>3</sup> have successfully implemented an optical probe traverse in the circumferential direction. Implementation of the traverse of a much smaller probe in the radial direction should be easier.

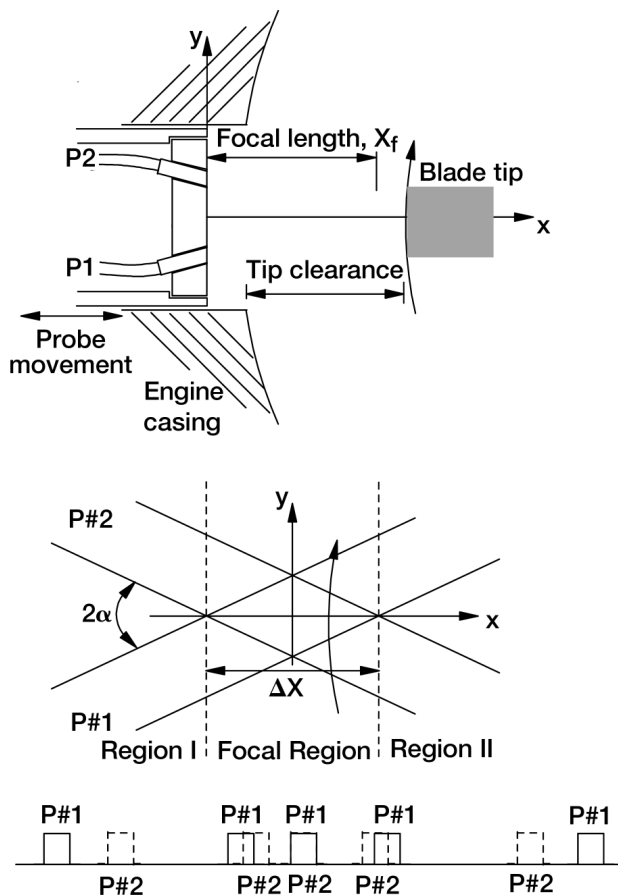


Figure 11.—Schematic of a scanning tip clearance probe and associated voltage pulses at various radial distances.

The advantage of the scanning optical tip-clearance sensor over the existing commercially available sensors, such as capacitive sensors, is that the tip clearance can be measured directly. Its disadvantage is that it requires actuation. However, because for accurate measurements, calibrations are usually required for the capacitive sensors, the added complexity of incorporating probe actuation is likely to be less costly than running a sensor calibration test. The scanning probe can also be used to calibrate a capacitance probe or a time-of-flight tip-clearance probe in-situ, if high accuracy is desired, and the installation of the scanning probe is not feasible because of spatial restrictions.

Another advantage of a scanning tip clearance probe over a time-of-flight probe is that pulse coincidence does not necessarily have to rely precisely on any particular trigger point, regardless how it is defined, but rather on minimizing the combined width of the two pulses collected during a probe traverse. It is therefore anticipated that the measurement with this probe could be made to be less prone to errors caused by surface imperfections. It also may prove advantageous to employ a coincidence-detection algorithm that relies on pulse-width comparison involving a series of points from rising and falling slopes of both pulses.

### Concluding Remarks

Initial application of the Time-of-Flight probe indicates that with further development it will likely offer a viable, and in some cases advantageous, alternative to the currently available tip clearance probes. Within the range of practical tip-clearance gaps its response is linear, and once its characteristics are established, calibration of the probe may not be necessary for a broad scope of applications. It is likely that with additional development the current accuracy of  $\pm 0.127$ -mm ( $\pm 0.005$ -in) will be improved.

### References

<sup>1</sup>Dhadwal, H.S., and Kurkov, A.P., 1998, "Dual-Laser Probe Measurement of Blade-Tip Clearance," American Society of Mechanical Engineers Paper 98-GT-183, June 1998.

<sup>2</sup>Dhadwal, H.S., Mehmud, A., Khan, R., and Kurkov, A.P., "Integrated fiber optic light probe: Measurement of static deflections in rotating turbomachinery," Rev. Sci. Instrum., Vol. 67 (2), 1996.

<sup>3</sup>Kurkov A.P., and Dhadwal H.S., "Simultaneous Optical Measurements of Axial and Tangential Steady-State Deflections" American Society of Mechanical Engineers Paper 99-GT-310, June 1999.

REPORT DOCUMENTATION PAGE			Form Approved OMB No. 0704-0188	
Public reporting burden for this collection of information is estimated to average 1 hour per response, including the time for reviewing instructions, searching existing data sources, gathering and maintaining the data needed, and completing and reviewing the collection of information. Send comments regarding this burden estimate or any other aspect of this collection of information, including suggestions for reducing this burden, to Washington Headquarters Services, Directorate for Information Operations and Reports, 1215 Jefferson Davis Highway, Suite 1204, Arlington, VA 22202-4302, and to the Office of Management and Budget, Paperwork Reduction Project (0704-0188), Washington, DC 20503.				
1. AGENCY USE ONLY (Leave blank)		2. REPORT DATE May 1999		3. REPORT TYPE AND DATES COVERED Technical Memorandum
4. TITLE AND SUBTITLE  Time-of-Flight Tip-Clearance Measurements			5. FUNDING NUMBERS  WU-538-03-11-00	
6. AUTHOR(S)  H.S. Dhadwal, A.P. Kurkov, and D.C. Janetzke				
7. PERFORMING ORGANIZATION NAME(S) AND ADDRESS(ES)  National Aeronautics and Space Administration John H. Glenn Research Center at Lewis Field Cleveland, Ohio 44135-3191			8. PERFORMING ORGANIZATION REPORT NUMBER  E-11692	
9. SPONSORING/MONITORING AGENCY NAME(S) AND ADDRESS(ES)  National Aeronautics and Space Administration Washington, DC 20546-0001			10. SPONSORING/MONITORING AGENCY REPORT NUMBER  NASA TM-1999-209183 AIAA-99-2134	
11. SUPPLEMENTARY NOTES  Prepared for the 35th Joint Propulsion Conference & Exhibit sponsored by AIAA ASME, SAE, and ASEE, Los Angeles, California, June 20-24, 1999. H.S. Dhadwal, Integrated Fiber Optic Systems, Inc., Stony Brook, New York; A.P. Kurkov and D.C. Janetzke, NASA Glenn Research Center. Responsible person, A.P. Kurkov, organization code 5930, (216) 433-5695.				
12a. DISTRIBUTION/AVAILABILITY STATEMENT  Unclassified - Unlimited Subject Categories: 35 and 06  This publication is available from the NASA Center for AeroSpace Information, (301) 621-0390.			12b. DISTRIBUTION CODE	
13. ABSTRACT (Maximum 200 words)  In this paper a time-of-flight probe system incorporating the two integrated fiber optic probes which are tilted equally relative to the probe holder centerline, is applied for the first time to measure the tip clearance of an advanced fan prototype. Tip clearance is largely independent of the signal amplitude and it relies on timing measurement. This work exposes optical effects associated with the fan blade stagger angle that were absent during the original spin-rig experiment on the zero stagger rotor. Individual blade tip clearances were measured with accuracy of $\pm 0.127$ -mm ( $\pm 0.005$ -in). Probe features are discussed and improvements to the design are suggested.				
14. SUBJECT TERMS  Optical measurement; Nonintrusive measurement; Turbomachinery blades			15. NUMBER OF PAGES 12	
			16. PRICE CODE A03	
17. SECURITY CLASSIFICATION OF REPORT Unclassified	18. SECURITY CLASSIFICATION OF THIS PAGE Unclassified	19. SECURITY CLASSIFICATION OF ABSTRACT Unclassified	20. LIMITATION OF ABSTRACT	